Received: 30 July 2020 | Revised: 23 July 2021 | Accepted: 8 September 2021

DOI: 10.1002/oca.2796

SPECIAL ISSUE ARTICLE

WILEY

Optimization of time-varying feedback controller parameters for freeway networks

Cecilia Pasquale | **Simona Sacone** | **Silvia Siri**

Department of Informatics, Bioengineering, Robotics and Systems Engineering, University of Genova, Genova, Italy

Correspondence
Cecilia Pasquale, Department of Informatics, Bioengineering, Robotics and Systems Engineering, University of Genova, Via Opera Pia 13, 16145 Genova, Italy.
Email: cecilia.pasquale@edu.unige.it

Abstract

In this work, a freeway traffic control scheme is proposed to regulate traffic in freeway networks via multi-class ramp metering. Specifically, each controlled on-ramp of the system adopts a feedback regulator of proportional-integral type and is able to compute the traffic flows entering the freeway mainstream, differentiated for each class of vehicles, e.g., cars and trucks. Since a crucial aspect of proportional-integral controllers is the tuning of parameters, in this work an optimization-based procedure is devised to determine the controller parameters to be used in the different on-ramps of the network, according to the detected traffic conditions. To this end, a set of representative traffic scenarios is defined and, for each scenario, an offline optimization procedure is applied to determine the optimal parameters. Then, in real time, a controller parameter selector identifies the scenario associated with the current system conditions and communicates to the local controllers the optimal parameters to be applied. The effectiveness of the proposed control scheme is tested in a simulative example and the main results are discussed in the paper.

KEYWORDS

feedback controller, freeway networks, optimization, traffic control

1 | INTRODUCTION

In a world in which individual mobility needs are becoming more and more pressing and road transport, both for freight and for passengers, keeps increasing, the efficient management of traffic networks is a fundamental topic to which researchers continue to devote important efforts to find solutions that combine economic needs, users' levels of service, efficiency, and environmental protection. Freeway systems, although designed to handle high volumes of traffic, are the infrastructures that have been mostly affected by the increase of traffic flows. The difficulty in managing the current traffic volumes, of both cars and trucks, is often due to structural shortcomings that cannot be easily solved, both for economic constraints and for physical limitations. In these circumstances, the development and the adoption of specific traffic controllers is the most effective way to improve the performance of freeway traffic systems.

In the past years, various control measures have been developed in order to allow for the efficient exploitation of transport infrastructures by making use of modern information and communication systems.[1] Among these, one of the

most widespread is ramp metering which, in real time and on the basis of the state measurements in the mainstream, modulates the traffic flows entering the freeway with the aim of reducing congestion, or with other objectives, such as minimizing emissions and crash risks, among others. In practical terms, applying ramp metering means defining the traffic volumes that can enter the on-ramps and translating them into appropriate traffic light cycles (an overview of the most common ramp metering implementation policies is given in Reference 2).

From a methodological point of view, the determination of the on-ramp flows can be carried out through different methodologies. Several approaches can be found in the literature, ranging from the application of feedback regulators to more sophisticated control strategies involving the solution of optimization problems, the definition of heuristic algorithms, or the development of hierarchical control schemes (for a complete overview see Reference 3). All these methods have proven to be capable of counteracting the onset of congestion with different levels of effectiveness by showing advantages and disadvantages, as briefly outlined below.

The most sophisticated control strategies are those based on the adoption of optimal control schemes. These frameworks appear in various forms within the literature where they are used based on the solution of finite horizon optimization problems[4-6] or defined as Model Predictive Control schemes.[7-10] In the freeway traffic control domain, the optimal control problems are generally characterized by a non-linear and non-convex structure which, combined with the large-scale nature of the system to be controlled, makes such problems generally difficult to be solved. One of the most effective methodologies for solving optimal control problems arising in the context of freeway traffic systems is the feasible direction algorithm, based on gradient calculation.[11] In case the calculation of the gradient becomes too demanding or even impossible, derivative-free algorithms can be applied to find the numerical solutions of the optimal control problems.[12] Although very effective in theory, the application of optimization-based methodologies in real freeway traffic systems is still rather limited, and this is mainly due to the high computational effort associated with the solution of these optimal control problems. To address this issue, several optimization-based control schemes have been specifically designed to reduce the computational effort, leading for instance to hierarchical control schemes[13] or distributed control schemes.[14] Yet, in the perspective of reducing the computational effort, other approaches involve the transformation of nonlinear traffic models into linear parameter varying models.[15,16]

As an alternative to optimization-based approaches, feedback regulators are often applied to compute ramp metering flows. Compared with optimization-based control schemes, they generally provide a less performing solution but present fewer limitations of practical applicability. These feedback control strategies are generally based on the definition of the desired traffic conditions and the implementation of control actions to keep the current traffic states close to predefined target values. Differently from optimal controllers, feedback regulators normally have a local nature, that is, the control actions are calculated on the basis of traffic measurements that are detected in an area close to the controlled on-ramps. The most famous feedback regulator for freeway systems is ALINEA,[17] which is an integral controller designed to improve the freeway throughput. An extension of ALINEA is given by PI-ALINEA,[18] including a proportional term in the control law, that has been proven to be more effective than ALINEA in stabilizing traffic conditions in presence of bottlenecks located far downstream the on-ramps.[19] Although the effectiveness of ALINEA and PI-ALINEA has been demonstrated in many real applications,[18] their ability to cope with congestion is inevitably affected by the typical limits of local control schemes in which the control action depends exclusively on the state measured in the immediate vicinity of the on-ramps. To overcome the local nature of classical feedback controllers, a proportional-integral feedback controller called *Extended Multi-class PI-ALINEA* (*EMC-PI-ALINEA*) has been proposed in References 20,21. As deeply analyzed in Reference 21, these types of controllers, which consider traffic measurements in wide road portions associated with each on-ramp, are more effective than traditional local PI regulators. However, a relevant issue associated with all feedback controllers concerns the tuning of the parameters characterizing the control law, that is, the gains and the reference value. Typically, these parameters are defined for a standard traffic scenario for which they prove to be effective, but, since in freeway networks the traffic conditions can change as a consequence of a wide combination of events, these standard parameters can result not to be completely effective in many cases.

In this paper, we propose a ramp metering control scheme designed to meet the real-time control requirements for large-scale traffic networks, in which the flows entering the on-ramps are computed through PI controllers whose control parameters are chosen according to the occurrence of different traffic scenarios and defined using an optimization-based procedure. Moreover, in this scheme the ramp metering controllers employed in each on-ramp have a multi-class nature and, therefore, specific control actions and control parameters are defined for different classes of vehicles (e.g., cars and trucks, for which the entering ramps are equipped with two separate lanes and signals). Some examples of multi-class

ramp metering can be found in References 6,22-25. However, as further clarified later on, the procedure here proposed has a general nature and can also be adopted to define the parameters of single-class feedback controllers.

In particular, the main features of the proposed control scheme are:

- the inflows, for each on-ramp and for each class of users, are computed with PI controllers;
- the parameters of the PI controllers can be different for each on-ramp and depend on the traffic conditions of the system; in particular, an *optimization procedure* is proposed to determine the parameters of the PI controllers according to a set of traffic scenarios; such optimization is realized offline for each scenario and a library of scenarios, each one characterized by a set of optimal control parameters, is created;
- a *controller parameter selector* is used to online identify the present scenario and, consequently, to select the optimal parameters for the PI controllers.

This scheme, with a few modifications, can be applied to optimally define the parameters of any PI feedback controller, in some way adapting such parameters to the traffic conditions in which they operate. For simplicity, in this paper we will explain the functioning of the control scheme using the *EMC-PI-ALINEA* controller as a PI controller. Through the simulation results we will demonstrate the versatility of the proposed scheme by applying it to optimally decide the parameters not only of *EMC-PI-ALINEA* controllers but also of *Multi-class PI-ALINEA* controllers.[26]

It is worth noting that the idea of optimizing the controller parameters on the basis of real-time traffic conditions has already been applied in the context of traffic control systems. For example, in Reference 27, the parameters of the perimeter-control regulator are updated in real-time based on traffic measurements, by exploiting machine learning techniques and adaptive optimization principles. In Reference 28, a modification of ALINEA is proposed in which the density set-point is time-varying and computed online on the basis of measurements of speeds and flows upstream the bottleneck. In Reference 29, a receding-horizon parametrized traffic control approach is considered, in which parametrized control laws are identified and the controller optimizes the parameters of such control law. Parametrized control laws are also considered in Reference 30, where the receding horizon control approach is scenario-based, that is, it optimizes the worst case among a set of scenarios in order to handle uncertainties. Compared with such approaches, in which the parameter optimization is realized in real time, the present work aims at reducing the computational effort by computing the controller parameters completely offline for each scenario, so that the only effort to be made online corresponds to choose the present scenario and the associated set of parameters. Indeed, one of the purposes of this work is to demonstrate the convenience of using optimization-based approaches within a scheme specifically developed to meet practical applicability requirements. As mentioned above, optimal control schemes often do not find application in real-world contexts both because of the high computational burden and because of the nonlinearity of the problems to be solved that prevents from easily finding a global optimal solution. The simulation results reported in this paper show that, by applying the optimization-based procedure to define the control parameters, the performance of the controllers is significantly increased. Moreover, the results produced by the application of the control scheme proposed in this paper are compared with those resulting from the solution of a finite-horizon optimal control problem. From this comparison, it can be observed that the application of the proposed control scheme, both using *EMC-PI-ALINEA* controllers and *Multi-class PI-ALINEA* controllers, produces results slightly worse than those obtained by solving the optimal control problem but with a computational effort that is much lower.

The paper is organized as follows. Section 2 describes the multi-class traffic flow model used in the optimization module. Section 3 presents the proposed control scheme, which is composed of the *EMC-PI-ALINEA* controllers, the optimization-based module and the controller parameter selector. In Section 4, the proposed control scheme is assessed in a simulation environment, considering the application to a test case. Conclusive remarks and some insights are finally given in Section 5.

2 | THE MULTI-CLASS METANET TRAFFIC FLOW MODEL

The optimization module included in the control scheme proposed in this paper is based on the predictive capabilities of a traffic flow model. In particular, the dynamic behavior of traffic is represented with a macroscopic and multi-class traffic

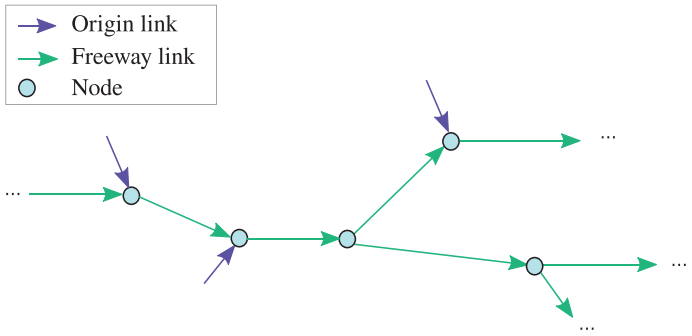

FIGURE 1 Links and nodes in the METANET model

flow model previously presented in Reference 23. This model is inspired by the well-known METANET model,[31] in its destination-oriented version, and extended to represent different classes of vehicles, specifically cars and trucks. Indeed, in case a high number of trucks is present in the freeway, they strongly affect the dynamics of the traffic system and the typical assumption that vehicles form a homogeneous stream is no longer valid. The larger size and lower operating capacity of trucks (lower speeds and longer reaction times) as well as the psychological impact that these vehicles have on the other drivers provoke slowdowns and even traffic jams if the presence of these vehicles is particularly high. In addition, the possibility of modeling the behavior of different classes of vehicles also allow to represent and then control the fluctuations in demand that may occur with different characteristics (in terms of duration, intensity, location in time and space) for such classes.

Let us now introduce the multi-class METANET traffic flow model, in which the freeway network is represented by means of a directed graph, composed of M freeway links, O origin links, and N nodes (see Figure 1). Each freeway link m is further divided into N_m sections with length L_m and λ_m lanes. The set of destinations reachable from link m is denoted with J_m, the set of destinations reachable from origin link o is denoted with $\bar{J}_o$, while the set of origin links that are controlled on-ramps is denoted with $\overline{O} \subseteq \{1, \dots, O\}$. For each node n, $\bar{\bar{J}}_n$ indicates the set of reachable destinations, O_n represents the set of exiting links, and $I_n/\bar{I}_n$ denote the set of entering freeway links/origin links. The multi-class METANET traffic flow model is a discrete model, that is, the time horizon is divided into K time steps, with sample time interval T [h]. Moreover, C vehicle classes are considered, with ς^c representing a conversion factor of vehicles of class c in Passenger Car Equivalent (PCE).

The variables referring to the freeway links are: $\rho^c_{m,i,j}(k)$ is the partial traffic density of class c in section i of link m at time instant kT with destination $j \in J_m$ [veh of class c/km/lane], $\rho^c_{m,i}(k)$ is the traffic density of class c in section i of link m at time instant kT [veh of class c/km/lane]; $\rho_{m,i}(k)$ is the total traffic density in section i of link m at time instant kT [PCE/km/lane]; $v^c_{m,i}(k)$ is the mean traffic speed of class c in section i of link m at time instant kT [km/h]; $q^c_{m,i}(k)$ is the traffic volume of class c leaving section i of link m during time interval $[kT, (k+1)T)$ [veh of class c/h]; $\gamma^c_{m,i,j}(k)$ is the portion of the traffic volume of class c in section i of link m at time instant kT having destination $j \in J_m$ (composition rate).

The variables referring to the origin links are: $d^c_{o,j}(k)$ is the partial origin demand of class c entering origin link o at time instant kT with destination $j \in \bar{J}_o$ [veh of class c/h]; $d^c_o(k)$ is the origin demand of class c entering origin link o at time instant kT [veh of class c/h]; $l^c_{o,j}(k)$ is the partial queue length of class c at origin link o with destination $j \in \bar{J}_o$ at time instant kT [veh of class c]; $l^c_o(k)$ is the queue length of class c at origin link o at time instant kT [veh of class c]; $\gamma^c_{o,j}(k)$ is the portion of the traffic volume of class c leaving origin link o at time instant kT having destination $j \in \bar{J}_o$ (composition rate); $\theta^c_{o,j}(k)$ is the portion of the demand of class c originating in origin link o at time instant kT having destination $j \in \bar{J}_o$; $q^c_o(k)$ is the traffic volume of class c leaving origin link o during time interval $[kT, (k+1)T)$ [veh of class c/h]; $q_o(k)$ is the total traffic volume leaving origin link o during time interval $[kT, (k+1)T)$ [PCE/h].

The variables referring to the nodes are: $Q^c_{n,j}(k)$ is the flow of class c entering node n during time interval $[kT, (k+1)T)$ with destination $j \in \bar{\bar{J}}_n$ [veh of class c/h]; $\beta^c_{m,n,j}(k)$ is the splitting rate, that is, the portion of the traffic volume present in node n at time instant kT which chooses link m to reach destination $j \in \bar{\bar{J}}_n$.

The two dynamic equations for the freeway links are referred to the two system state variables, that are the partial traffic density and the mean speed, that is,

$$\rho^c_{m,i,j}(k+1) = \rho^c_{m,i,j}(k) + \frac{T}{L_m \lambda_m}\left[\gamma^c_{m,i-1,j}(k) q^c_{m,i-1}(k) - \gamma^c_{m,i,j}(k) q^c_{m,i}(k)\right] \tag{1}$$

$$v^c_{m,i}(k+1) = v^c_{m,i}(k) + \frac{T}{\tau^c}\left[V^c(\rho_{m,i}(k)) - v^c_{m,i}(k)\right] + \frac{T}{L_m} v^c_{m,i}(k)\left[v^c_{m,i-1}(k) - v^c_{m,i}(k)\right] - \frac{\nu^c T\left[\rho_{m,i+1}(k) - \rho_{m,i}(k)\right]}{\tau^c L_m\left[\rho_{m,i}(k) + \chi^c\right]} \tag{2}$$

$c = 1, \dots, C,\ m = 1, \dots, M,\ i = 1, \dots, N_m,\ j = 1, \dots, J_m,\ k = 0, \dots, K-1$. The steady-state speed-density relation $V^c(\rho_{m,i}(k))$ and the traffic volume $q^c_{m,i}(k)$ in (2) are respectively obtained as

$$V^c(\rho_{m,i}(k)) = v^{\mathrm{f},c}_{m,i} \cdot \left[1 - \left(\frac{\rho_{m,i}(k)}{\rho^{m,i}_{\max}}\right)^{l^c}\right]^{m^c} \tag{3}$$

$$q^c_{m,i}(k) = \rho^c_{m,i}(k) v^c_{m,i}(k) \lambda_m \tag{4}$$

where $\rho_{m,i}(k) = \sum_{c=1}^{C} \varsigma^c \rho^c_{m,i}(k)$, while $v^{\mathrm{f},c}_{m,i}$ is the free-flow speed in section i of link m for class c [km/h], $\rho^{\max}_{m,i}$ is the jam density in section i of link m [PCE/km/lane].

The dynamic equation for the origin links is a conservation equation for the queue lengths, which are other state variables, given by

$$l^c_{o,j}(k+1) = l^c_{o,j}(k) + T\left[d^c_{o,j}(k) - \gamma^c_{o,j}(k) q^c_o(k)\right] \tag{5}$$

$c = 1, \dots, C$, $o = 1, \dots, O$, $j = 1, \dots, \bar{J}_o$, $k = 0, \dots, K-1$, in which the traffic flow $q^c_o(k)$, that is, the traffic flow of class c leaving origin link o, having m as downstream link, is computed in a different way if the origin link o is a controlled on-ramp or not. Hence, it is possible to write:

$$q^c_o(k) = \min\left\{d^c_o(k) + \frac{l^c_o(k)}{T}, q^{\max,c}_o, q^{\max,c}_o \cdot \frac{\rho^{\max}_{m,1} - \rho_{m,1}(k)}{\rho^{\max}_{m,1} - \rho^{\mathrm{cr}}_{m,1}}\right\} \qquad o \notin \overline{O} \tag{6}$$

$$q^c_o(k) = \min\left\{d^c_o(k) + \frac{l^c_o(k)}{T}, q^{\max,c}_o, \overline{q}^c_o(k), q^{\max,c}_o \cdot \frac{\rho^{\max}_{m,1} - \rho_{m,1}(k)}{\rho^{\max}_{m,1} - \rho^{\mathrm{cr}}_{m,1}}\right\} \qquad o \in \overline{O} \tag{7}$$

where $q^{\max,c}_o$ is the maximum flow of class c in origin link o, $\rho^{\mathrm{cr}}_{m,1}$ is the critical density of the first section of link m [PCE/km/lane], and $\overline{q}^c_o(k)$ is the ramp-metering control variable, that is, the on-ramp flow computed by the controller for class c.

Moreover, the incoming traffic flow in a given node and the traffic flow entering the first section of a link exiting a node are computed, respectively, as

$$Q^c_{n,j}(k) = \sum_{\mu \in I_n} q^c_{\mu,N_\mu}(k) \gamma^c_{\mu,N_\mu,j}(k) + \sum_{o \in \bar{I}_n} q^c_o(k) \gamma^c_{o,j}(k) \tag{8}$$

$$q^c_{m,0}(k) = \sum_{j \in J_m} \beta^c_{m,n,j}(k) \cdot Q^c_{n,j}(k) \tag{9}$$

3 | THE PROPOSED CONTROL FRAMEWORK

The traffic control scheme proposed in this paper aims at regulating a freeway network via multi-class ramp metering in order to counteract the traffic congestion that may arise as a consequence of high traffic volumes. This control scheme

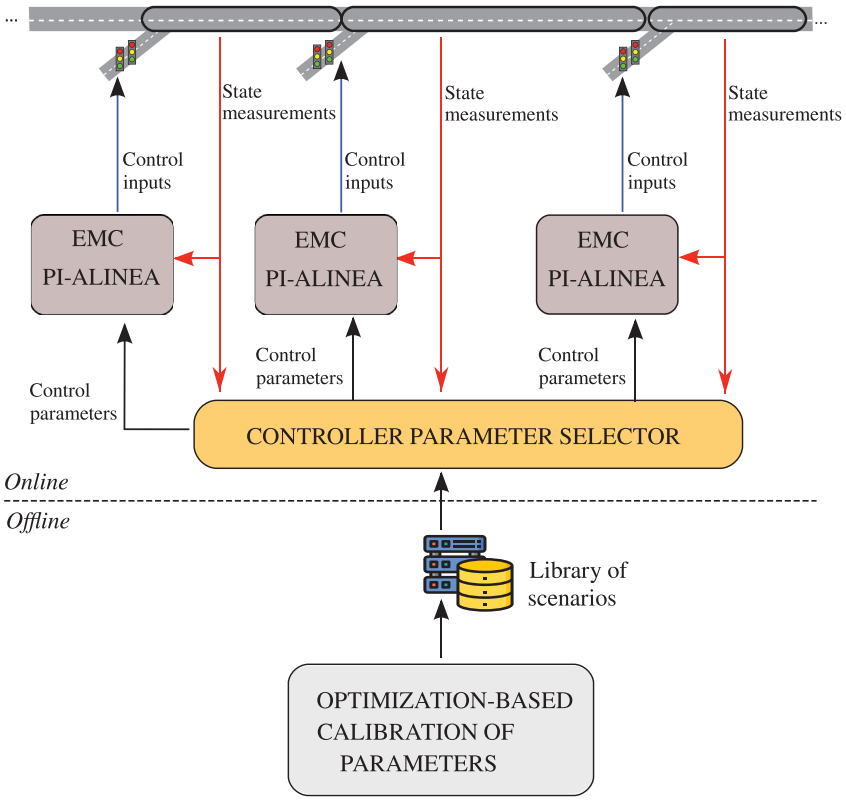

FIGURE 2 The proposed control framework

is designed to combine the requirements of practical applicability (low computational effort and simple controller structure) with the need to ensure high performance in the presence of different traffic scenarios, due to both recurrent and non-recurrent traffic conditions. As specified in the Introduction, this control scheme can include several types of PI controllers. In this section, the scheme in which each controlled ramp is equipped with an *EMC-PI-ALINEA* controller is presented. Specifically, as sketched in Figure 2, this control framework is composed of three main components, the *EMC-PI-ALINEA* controllers and the control parameter selector, which act online, and the optimization-based calibration of parameters, which is a procedure applied completely offline. The main features of these components are briefly sketched below and, then, described in the following subsections:

- the *EMC-PI-ALINEA* controllers are present in each controlled on-ramp and compute the control actions on the basis of the measurements collected in a neighborhood of the on-ramp itself: the parameters of each controller are time-varying, that is, they change according to the current scenario detected in real time by the control parameter selector;
- the *control parameter selector* is the module of the control scheme which decides the parameters to be transmitted to each *EMC-PI-ALINEA* controller; this block receives the state measurements from the real system and other information from the traffic manager and, on the basis of this real-time knowledge, chooses from the library of traffic scenarios the most suitable one and transmits to the *EMC-PI-ALINEA* controllers the associated parameters;
- the *optimization-based calibration of parameters* is an optimization procedure applied offline which computes, for each traffic scenario, the corresponding set of optimal values of the *EMC-PI-ALINEA* parameters.

3.1 | The EMC-PI-ALINEA controllers

In each controlled on-ramp, an *EMC-PI-ALINEA* controller operates referring to a neighborhood of the on-ramp, called *action area* of the on-ramp. This area corresponds to a set of road sections and links which are located between two consecutive on-ramps. In particular, referring to a generic controlled origin link $o \in \overline{O}$, let I_o^{act} and M_o^{act} denote the set

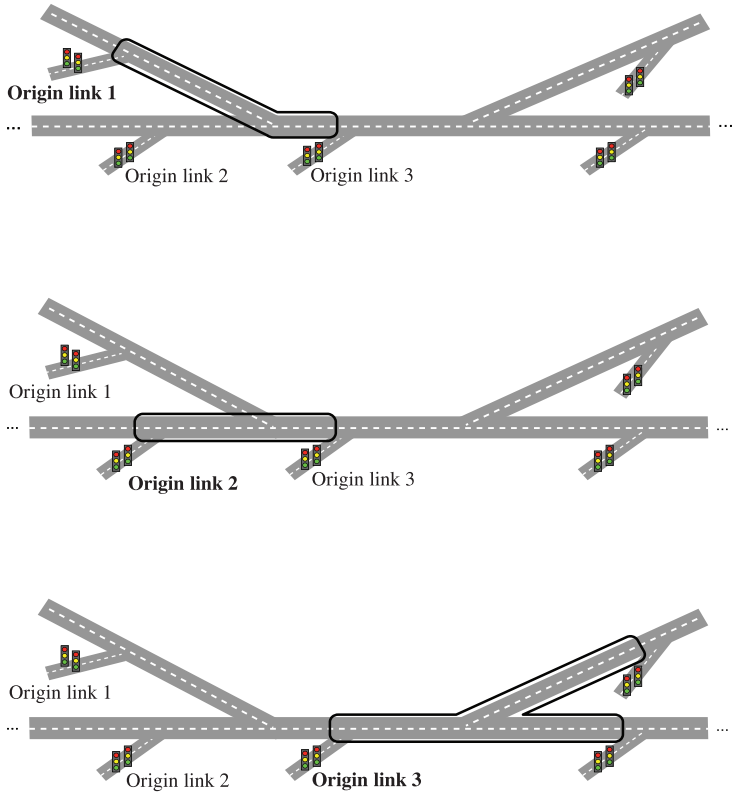

FIGURE 3 Example of action areas

of sections and the set of links corresponding to the action area of origin link o. On the basis of the measurements taken within the action area associated with each controlled on-ramp, the *EMC-PI-ALINEA* controllers calculate the corresponding control laws.

An example to clarify the concept of action area is reported in Figure 3, where the action area for origin links 1, 2, and 3 are shown with reference to a simple freeway network. It is worth noting that the size of each action area depends on the geometry of the freeway network and, as in the case of origin links 1 and 2 in this example, it may happen that two action areas overlap. Also, in case of a bifurcation in the road network, the action area of an on-ramp can include a set of road sections that are not contiguous but correspond to the diverging paths.

Considering a generic origin link $o \in \overline{O}$, the *EMC-PI-ALINEA* controller computes the flow of each class c of vehicles that should enter in the mainstream at time step k from link o according to the following control law:

$$\overline{q}_o^c(k) = \max\{q_o^{\min,c}, q_o^c(k-1) - K_{\mathrm{P},o}^{c,\sigma}[\rho_{m,1}^c(k) - \rho_{m,1}^c(k-1)] + K_{\mathrm{R},o}^{c,\sigma} \cdot f_o^{c,\mathrm{act}}(k)[\hat{\rho}_o^\sigma - \rho_o^{\mathrm{act}}(k)]\} \tag{10}$$

where:

- $q_o^{\min,c}$ is the minimum traffic volume for class c in origin link o;
- $f_o^{c,\mathrm{act}}(k)$ is a weighted ratio used to properly split the entering flow among the different vehicle classes; more specifically, $f_o^{c,\mathrm{act}}(k)$ is computed at each time step k and provides the ratio of the number of vehicles of class c over all the vehicles present in the origin link o and in the sections belonging to the action area of link o, that is,

$$f_o^{c,\mathrm{act}}(k) = \frac{\varsigma^c \eta_o^c(k)}{\sum_{h=1}^{C} \varsigma^h \eta_o^h(k)} \tag{11}$$

where $\eta_o^c(k)$ is given by

$$\eta_o^c(k) = l_o^c(k) + \sum_{m \in M_o^{\mathrm{act}}(k)} \sum_{i \in I_o^{\mathrm{act}}(k)} L_m \rho_{m,i}^c(k) \tag{12}$$

- $\rho_o^{\text{act}}(k)$ is the highest total density detected in the action area associated with on-ramp o, that is,

$$\rho_o^{\text{act}}(k) = \max_{m \in M_o^{\text{act}}(k), i \in I_o^{\text{act}}(k)} \rho_{m,i}(k) \tag{13}$$

  considering the highest value of the density in the action area to be compared with the set-point corresponds to refer to the worst case and, then, to apply a ramp-metering controller that is able to react immediately when a congestion appears;
- $K_{\text{P},o}^{c,\sigma}$, $K_{\text{R},o}^{c,\sigma}$, and $\hat{\rho}_o^{\sigma}$ are the parameters of the controller and represent, respectively, the proportional/integral gains and the total density set-point for the action area associated with the current scenario σ.

As specified earlier, the controller parameters $K_{\text{P},o}^{c,\sigma}$, $K_{\text{R},o}^{c,\sigma}$ and $\hat{\rho}_o^{\sigma}$ are time-varying and communicated by the control parameter selector that chooses the optimal values of these parameters associated with the current scenario σ. Note that the gains $K_{\text{P},o}^{c,\sigma}$ and $K_{\text{R},o}^{c,\sigma}$ are different for each origin link o and for each class c, while the density set-point $\hat{\rho}_o^{\sigma}$ refers to the overall traffic density and only varies with the origin link o.

Moreover, the control actions (10) are referred to the specific classes of vehicles but are computed by measuring the overall density inside road sections, thus considering the contemporary presence in the freeway links of vehicles belonging to different categories. Finally, it is worth noting that both $f_o^{c,\text{act}}(k)$ in (11) with (12) and $\rho_o^{\text{act}}(k)$ in (13) are computed considering the measurements in the overall action area, in this way the ramp metering control law is able to react more in advance compared to the case of local controllers based only on one measurement close to the on-ramp.

3.2 | Optimization-based calibration of parameters

In the proposed control scheme, the controller parameters vary for each origin link and, also, depending on the considered traffic conditions. The need to consider different parameters for different origin links is related to the fact that, in a large scale network (e.g., containing links with different length and slope or with multiple merging zones or bifurcations), the characteristics of the road may differ significantly in different areas as well as some local events can have impact only in specific areas. Moreover, recurrent or non-recurrent fluctuations in the traffic demand and the occurrence of exceptional events such as road accidents, road works, or bad weather conditions may require the change of the controller parameters over time. These different traffic conditions are captured in the proposed control scheme in terms of *traffic scenarios*.

Specifically, let Σ denote the set (library) of considered traffic scenarios. Each traffic scenario $\sigma \in \Sigma$ is characterized by a set $\mathbb{P}^{\sigma}$ of data and a set $\mathbb{K}^{\sigma}$ of controller parameters. The set $\mathbb{P}^{\sigma}$ includes the model parameters and the features of the scenario, that are used in the optimization procedure. On the other hand, the set $\mathbb{K}^{\sigma}$ includes the controller parameters that are obtained as a result of the optimization procedure and then used by the *EMC-PI-ALINEA* controllers.

The considered scenarios are associated with both recurrent traffic conditions and non-recurrent situations:

- in *recurrent* conditions, each scenario refers to a given time window (e.g., morning peak hour) together with the corresponding features, such as the traffic demand; note that different scenarios are considered for working and non-working days;
- *non-recurrent* conditions correspond either to capacity reductions caused by accidents/road works or to traffic peaks due to exceptional events; such peaks can be referred to a specific vehicle class or the total traffic flow; non-recurrent conditions are differentiated depending on time windows and type of day, analogously to recurrent conditions. Moreover, it is assumed that there are not capacity reductions/traffic peaks simultaneously happening in different action areas of the freeway network.

The set of traffic scenarios must be customized for the considered traffic network on the basis of historical data; moreover, the library of scenarios can be updated from time to time when new traffic conditions become relevant enough to be classified as a new scenario. Then, it is necessary to start with a base library that may also contain a limited number of scenarios including at least the recurrent conditions of a representative working day and of a representative non-working day. The duration of the time windows, and thus the number of scenarios to be included in the library, depends on the

characteristics of the traffic demand of the considered network. In particular, the duration can vary from 2 to 4 h for daytime scenarios, while it can be more extended for night scenarios, ranging from 6 to 8 h, yielding about 6-10 scenarios per day. As for non-recurring scenarios, these can be defined based on historical data or reproduced using a dynamic traffic model. For instance, in the case of planned roadworks in which the capacity of a freeway stretch is expected to be temporarily reduced, the model presented in Section 2 can be used to reproduce the scenarios associated with this event.

The set $\mathbb{P}^\sigma$ of data associated with scenario σ is given by

$$\mathbb{P}^\sigma = \{k_0^\sigma, H^\sigma, I^\sigma, D^\sigma, M^\sigma\} \tag{14}$$

where k_0^σ is the starting time step, H^σ is the length of the time horizon, $I^\sigma = \{\rho^c_{m,i,j}(k_0^\sigma), v^c_{m,i}(k_0^\sigma),\ \forall c, \forall m, \forall i, \forall j, l^c_{o,j}(k_0^\sigma), \forall c, \forall o, \forall j\}$ gathers the initial conditions of the state variables, $D^\sigma = \{d^{c,\sigma}_{o,j}(k), \forall c, \forall o, \forall j, k = k_0^\sigma, \dots, k_0^\sigma + H^\sigma - 1\}$ is the set of traffic demands, $M^\sigma = \{\rho^{\max,\sigma}_{m,i}, \lambda^\sigma_m, \forall m, \forall i\}$ includes the model parameters referred to the capacity configuration (in order to properly model situations of capacity reductions) in scenario σ.

The set $\mathbb{K}^\sigma$ is given by

$$\mathbb{K}^\sigma = \left\{K^{c,\sigma}_{\mathrm{P},o}, K^{c,\sigma}_{\mathrm{R},o}, \hat{\rho}^\sigma_o, \forall c, \forall o\right\} \tag{15}$$

that is, it is composed of the controller parameters present in the control law defined (10). The parameters gathered in $\mathbb{K}^\sigma$ and associated with each scenario σ are found by offline running an optimization-based procedure in which they are the decision variables to be found, while the objective function corresponds to the minimization of travel times for travelers. The problem constraints are given by the multi-class METANET traffic flow model described in Section 2. Hence, the optimization-based procedure exploits the predictive capabilities of the traffic flow model in order to determine the controller parameters that yield the optimal predicted dynamic behavior of the system during the whole time horizon in each scenario.

The general formulation of the optimization problem, referred to scenario σ, based on the set $\mathbb{P}^\sigma$ and aimed at the optimal calibration of controller parameters in $\mathbb{K}^\sigma$, is the following.

Problem 1. Given the system initial conditions I^σ, the demands D^σ and the set M^σ, find $\mathbb{K}^\sigma$ that minimizes

$$\mathcal{J} = T \sum_{k=k_0^\sigma}^{k_0^\sigma+H^\sigma} \sum_{c=1}^{C} \varsigma^c \left(\sum_{m=1}^{M} \sum_{i=1}^{N_m} L_m \rho^c_{m,i}(k) + \sum_{o=1}^{O} l^c_o(k) \right) \tag{16}$$

subject to (1)–(9), (10)–(13) and

$$\underline{K}_P \le K^{c,\sigma}_{\mathrm{P},o} \le \overline{K}_P, \qquad c = 1, \dots, C,\ o = 1, \dots, O \tag{17}$$

$$\underline{K}_R \le K^{c,\sigma}_{\mathrm{R},o} \le \overline{K}_R, \qquad c = 1, \dots, C,\ o = 1, \dots, O \tag{18}$$

$$\underline{\rho} \le \hat{\rho}^\sigma_o \le \overline{\rho}, \qquad o = 1, \dots, O \tag{19}$$

with $\underline{K}_P$, $\underline{K}_R$, $\underline{\rho}$ and $\overline{K}_P$, $\overline{K}_R$, $\overline{\rho}$, respectively, lower and upper bounds for the decision variables.

The objective function to be minimized in Problem 1 is the Total Time Spent, denoted also with *TTS* and measured in [PCE·h]. This index is a very common objective in traffic control problems and gives an indication of the time spent by all vehicles in the freeway system. As shown in (16), the Total Time Spent is obtained as the sum of the so-called Total Travel Time, that is, the time spent by vehicles traveling along the freeway and denoted with *TTT*, and the so-called Total Waiting Time, that is, the time spent by vehicles waiting in the origin links and denoted with *TWT*. Note that minimizing *TTS* means maximizing the system throughput and thus maximizing the system performance.

The constraints in Problem 1 are related to the dynamics of the controlled system (1)–(9), (10)–(13) and to lower and upper bounds for the values of the gains and set-point, as reported in (17)–(19). Note that the lower and upper

bounds of the decision variables must be properly defined since their values can affect the duration of the traffic light cycle.

Besides computing the parameters in $\mathbb{K}^\sigma$, the solution of Problem 1 also provides the optimal values of the state variables for the considered scenario σ. For such variables, the average values in time intervals of equal length (in which the horizon H^σ is discretized) are computed. More precisely, P^σ intervals are defined, with $P^\sigma < H^\sigma$, and the following values are obtained

$$\overline{\rho}^c_{m,i}(\kappa), \overline{v}^c_{m,i}(\kappa), \overline{l}^c_o(\kappa), \qquad \kappa = 1, \ldots, P^\sigma \tag{20}$$

and used by the controller parameter selector, as it will be described in Section 3.3.

It is worth noting that the dynamics of the traffic system described by the problem constraints (1)–(9) and (10)–(13) is nonlinear, hence Problem 1 is a nonlinear optimization problem. For the solution of this problem, we have adopted a gradient-free solution algorithm and, specifically, Simulated Annealing. *Simulated Annealing* is an iterative stochastic algorithm for global nonlinear optimization, first introduced in Reference 32, then extended to combinatorial optimization,[33] and to continuous optimization.[34] To perform a random search in the solution space, the Simulated Annealing algorithm is initialized with a feasible starting solution s_0 that is assigned to the current solution s, that is, $s = s_0$. At each iteration ι of the algorithm:

- a tentative solution s_ι (tentative values of the gain parameters and of the density set-points) in the neighborhood of the current solution s is generated;
- if the tentative solution is better than the current one, that is, $obj(s_\iota) < obj(s)$ (where $obj(\cdot)$ is the objective function associated with the solution), the tentative solution becomes the current solution, that is, $s = s_\iota$;
- if the tentative solution is worse than the current one, that is, $obj(s_\iota) \geq obj(s)$, the tentative solution is accepted as new current solution according to a probability given by $\exp\left(\frac{obj(s)-obj(s_\iota)}{\Gamma_\iota}\right)$. The parameter Γ_ι is called "temperature" by analogy with the annealing process and is updated with the iterations according to a suitable cooling schedule, so that the probability of accepting a worse solution decreases with the algorithm iterations. In particular, the cooling scheme proposed in Reference 35 is applied, that is, the temperature at iteration ι is obtained as $\Gamma_\iota = \left|\frac{obj(s)}{\log(P_\iota)}\right| \delta$, where δ represents the worsening percentage at each iteration and P_ι is the worsening reference acceptance probability, with $P_\iota = \alpha \cdot P_{\iota-1}$;
- the algorithm stops when $\iota = I^{max}$ or $\iota = I^{ni,max}$, with I^{max} being the maximum number of total iterations and $I^{ni,max}$ the maximum number of consecutive non-improving iterations.

3.3 | The controller parameter selector

The controller parameter selector acts online and chooses the set of parameters $\mathbb{K}^\sigma$ to be adopted by the local controllers on the basis of the present scenario σ. At the beginning of each time window for each type of day, this module changes the scenario referred to that time window in *recurrent* conditions. On the other hand, *non-recurrent* situations must be detected online depending on the type of condition:

- capacity reductions are communicated to the selector by the traffic manager; this communication can occur in advance, for example, in case of pre-scheduled road works, or in real time, for example, in case of traffic accidents;
- traffic peaks due to exceptional events are detected on the basis of the measured traffic state, compared with the average values of the state variables associated with the recurrent scenario of the same time window and type of day; in particular, at each time step k the following conditions are verified:

$$\rho^c_{m,i}(k) > \overline{\rho}^c_{m,i}(\kappa) + \Delta^\rho, \qquad \kappa = \left\lceil k / \frac{H^\sigma}{P^\sigma} \right\rceil \tag{21}$$

$$v^c_{m,i}(k) < \overline{v}^c_{m,i}(\kappa) + \Delta^v, \qquad \kappa = \left\lceil k / \frac{H^\sigma}{P^\sigma} \right\rceil \tag{22}$$

$$l^c_o(k) > \overline{l}^c_o(\kappa) + \Delta^l, \qquad \kappa = \left\lceil k / \frac{H^\sigma}{P^\sigma} \right\rceil \tag{23}$$

with Δ^{ρ}, Δ^{v} and Δ^{l} suitable tolerance values. If one of these conditions is verified for at least one vehicle class c, a section i of link m or an origin link o, a different scenario must be chosen. This scenario is the one corresponding to the present time window and type of day but with an increased demand profile. In case the detected scenario is completely new, that is, the corresponding parameters have not been computed yet, the present scenario corresponding to recurrent conditions is maintained and the parameters associated with the new scenario are computed off-line, so that they will be used in the future when this scenario will happen again.

Note that, alternatively to the procedure proposed in this article, the most suitable scenario can be also selected with more sophisticated methods, for example, based on classification techniques or clustering methods (see References 36-39).

4 | SIMULATIVE RESULTS

This section reports the results obtained by applying the control scheme proposed in Section 3. More in detail, the objective of this section is twofold: on the one hand, we want to show that the optimal setting of the controller parameters significantly affects the performance of the controllers and, on the other hand, we want to demonstrate the versatility of the proposed scheme by adopting two different PI controllers, namely the *Multi-class PI-ALINEA* and the *EMC-PI-ALINEA*, within the control framework introduced in Section 3. In addition, an optimization-based control approach is considered to further assess the effectiveness of the proposed control framework. Specifically, this section is further divided into three subsections: Section 4.1 describes the characteristics of the freeway network in use and the settings for creating the libraries of scenarios related to the two controllers. Section 4.2 analyzes in depth the traffic behavior in absence of control, while in Section 4.3 the results obtained with the application of several control strategies are illustrated and discussed. All results shown in this section were obtained using MATLABR2017b software on a MacBook Pro with a 2 GHz Intel Core i5 quad-core processor.

4.1 | Settings of the case study

Let us first describe the structure of the freeway network considered in this work and depicted in Figure 4. Such network consists of six freeway links, indicated with m1 to m6. Each link is composed of three lanes and a variable number of sections, each of which has a length of 800 [m]. The network also includes five origin links denoted with o1 to o5 and one exiting branch located between the origin links o2 and o3. Note that the origin links o2, o3, o5 are controlled and equipped with dedicated traffic lights for each class of vehicles, that is, o2, o3, o5 $\in \overline{O}$. Then, for each controlled origin link the corresponding action area has been individuated, as shown in Figure 4.

On the basis of such network, a library of traffic scenarios representing recurrent and non-recurrent traffic conditions has been created. For the purposes of this work, a working day has been considered in which eight time windows lasting 3 hours have been identified. This implies that each scenario, whether representing recurring or non-recurring conditions, has this duration. The behavior of each scenario has been simulated with the multi-class METANET model described in Section 2 considering a sample time T corresponding to 10 [s] that, for a total time horizon of 3 hours, yields $K = 1080$ time steps. The main model parameters common to each traffic scenario are reported in Table 1.

The library associated with the control scheme adopting *EMC-PI-ALINEA* controllers has been created for each scenario σ by solving Problem 1. To create the library in case *Multi-class PI-ALINEA* controllers are used, a slightly different

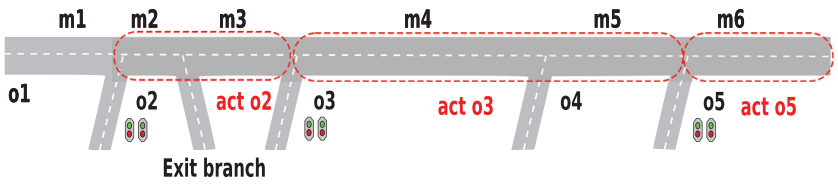

FIGURE 4 Layout of the freeway stretch with action areas (red dashed line)

TABLE 1 Main model parameters

Parameter	Value	Range
Multi-class traffic flow model		
$v_{m,i}^{\mathrm{f},1}$	120 [km/h]	$\forall m, \forall i$
$v_{m,i}^{\mathrm{f},2}$	90 [km/h]	$\forall m, \forall i$
$\rho_{m,i}^{\max}$	600 [PCE/km]	$\forall m, \forall i$
$q_o^{\max,1}$	1800 [veh/h]	$o \in \overline{O}$
$q_o^{\max,2}$	450 [veh/h]	$o \in \overline{O}$
$q_o^{\max,1}$	6000 [veh/h]	$o \notin \overline{O}$
$q_o^{\max,2}$	1500 [veh/h]	$o \notin \overline{O}$
ς^1	1 [PCE]	
ς^2	4 [PCE]	

control problem has been solved, that is, Problem 1 in which (10)–(13) are replaced by the Multi-class PI-ALINEA control law, given by:

$$\overline{q}_o^c(k) = \max\{q_o^{\min,c}, q_o^c(k-1) - K_{\mathrm{P},o}^{c,\sigma}[\rho_{m,1}^c(k) - \rho_{m,1}^c(k-1)] + K_{\mathrm{R},o}^{c,\sigma} \cdot f_o^c(k)[\hat{\rho}_o^\sigma - \rho_{m,1}^c(k)]\} \tag{24}$$

where the weighted ratio $f_o^c(k)$ is computed as

$$f_o^c(k) = \frac{\varsigma^c \cdot [\rho_{m,1}^c(k) L_m + l_o^c(k)]}{\sum_{c=1}^2 \varsigma^c \cdot [\rho_{m,1}^c(k) L_m + l_o^c(k)]} \tag{25}$$

The optimization problems have a time horizon $H^\sigma = 1080$, while the lower and upper bounds on the decision variables have been fixed as follows: $\underline{K}_P = 1$, $\underline{K}_R = 1$, $\underline{\rho} = 45$ [PCE/km] and $\overline{K}_P = 200$, $\overline{K}_R = 200$, $\overline{\rho} = 250$ [PCE/km]. The resulting optimization problems have been solved with the Simulated Annealing algorithm described in Section 3.2, in which the following values of the parameters have been fixed: $\delta = 0.01$, $P_0 = 0.6$, $\alpha = 0.9995$.

For each scenario belonging to each library, the Simulated Annealing algorithm has been initialized with different initial solutions. Furthermore, since the solution search procedure of the algorithm is randomized, the solution algorithm has been run several times for each instance, in order to choose the best solution to be included in the traffic scenario libraries. According to our results it seems that, for this optimization problem, the choice of the initial solution does not have a significant influence on the solution produced by the algorithm that always provides a set of parameters improving the objective function. In Figure 5 two examples of objective function trends during the optimization runs

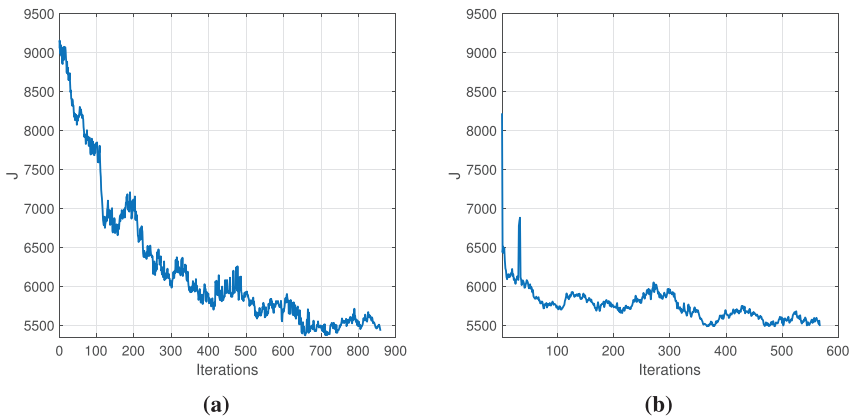

FIGURE 5 Examples of objective function trends in two optimization runs of the Simulated Annealing algorithm with different initial solutions

for the parameter definition of *EMC-PI-ALINEA* controllers are shown. Similar trends have been obtained for optimization problems in which the *Multi-class PI-ALINEA* control law has been applied. Note that the two trends in Figure 5 are characterized by two different initial solutions, but still reach a similar local minimum. As it can also be seen in Figure 5, the Simulated Annealing algorithm, by its intrinsic nature, admits the acceptance of worse solutions and it can, in some cases, increase the value of the objective function. However, in this work, the solution corresponding to the lowest value of the cost function is stored in memory and therefore it is used if, at the end of the solution procedure, the current solution is not the minimum one. Finally, note that the computational time to solve Problem 1 for this setting is of about 1 minute on a standard PC, hence absolutely acceptable taking into account that these optimization problems are solved offline.

4.2 | The uncontrolled case

Let us now introduce a case study concerning the freeway network previously described and specifically developed to test the capabilities of the proposed control scheme. In this section, only the behavior of the system without the application of any control measures is analyzed. This case study starts at 6 a.m. and lasts until 1 p.m. for a total duration of 7 [h] (corresponding to $K = 2500$ time steps), including both recurrent and non-recurrent traffic scenarios. Specifically, a data set that considers two types of vehicles, that is, cars and trucks, has been considered.

The profiles of traffic demand at the controlled on-ramps are reported in Figure 6 in which the blue line indicates the traffic demand of cars and the red line refers to the traffic demand of trucks. The first three hours represent a typical rush hour situation, while at 10:30 a.m. a traffic accident occurs causing the capacity reduction of a portion of freeway for about one hour. The freeway sections affected by the capacity reduction are located in the action area referred to origin link o2, immediately upstream of the freeway exit branch.

With these traffic inputs and considering the model settings previously introduced, the multi-class METANET model reproduces the traffic behavior of the freeway network, which can be summarized in the mainstream density evolution reported in Figure 7. Analyzing this figure, it is possible to observe that the uncontrolled case is characterized by the presence of two main congestions. The former involves the first three hours of the simulation and is due to a high transport demand of commuters, the freeway links more affected by this congestion being m3, m4, and m5. The latter congestion appears as a consequence of the traffic accident in the freeway link m2 and propagates backwards until link m1. The capacity reduction induced by the traffic accident has two main effects, namely obstructing the flow that wants to reach its destination far downstream and blocking the exit branch. Without applying any traffic control, the Total Time Spent *TTS* is equal to 10489 [PCE·h].

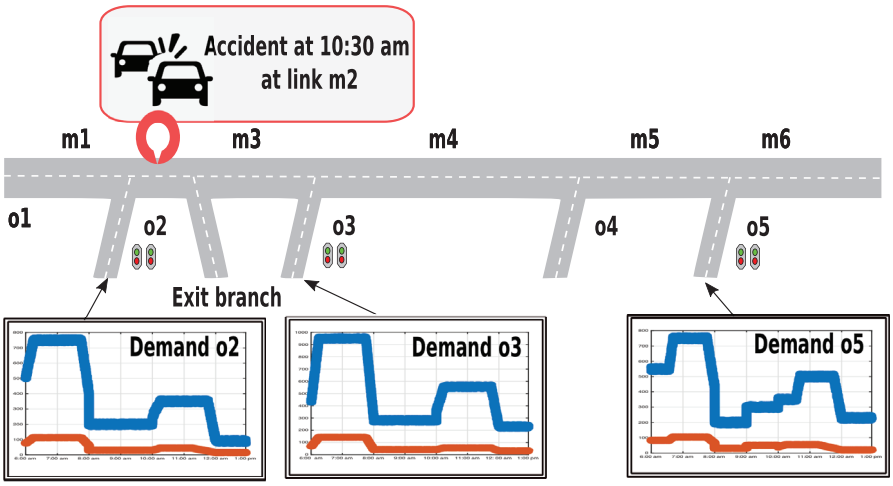

FIGURE 6 Traffic demands and location of the traffic accident in the considered freeway stretch

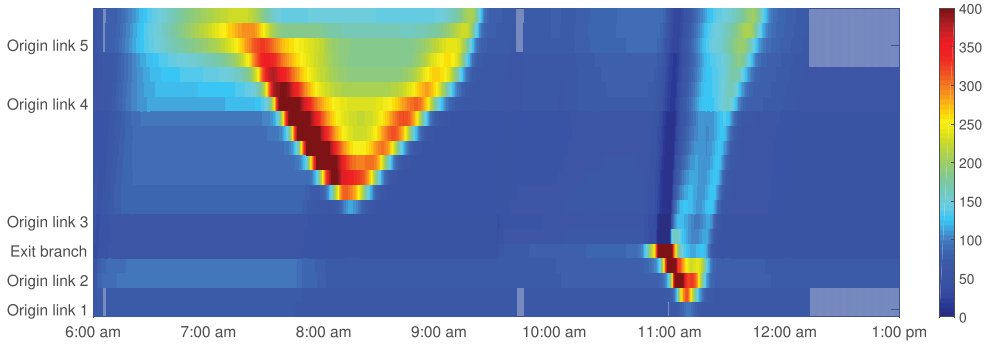

FIGURE 7 Traffic density evolution in time and space in the uncontrolled case

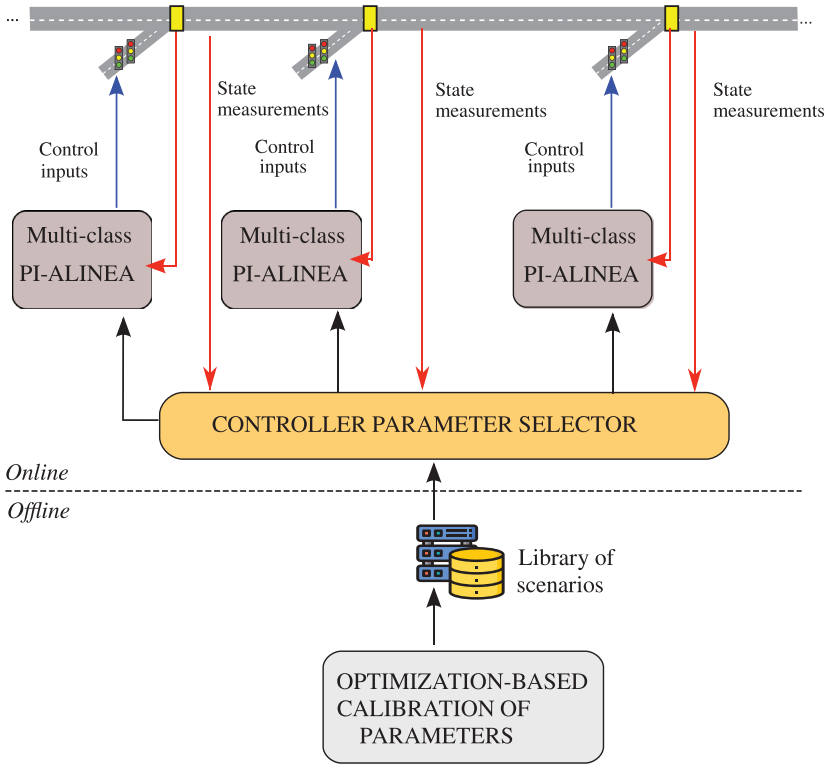

FIGURE 8 The control framework with *Multi-class PI-ALINEA* controllers

4.3 | The controlled cases

In this section the results obtained by applying four control strategies to the case study introduced in Section 4.2 are shown and discussed. More in detail, the adopted control schemes are:

Control scheme 1: standard *Multi-class PI-ALINEA* controllers are adopted with standard controller parameters taken from the literature;

Control scheme 2: *Multi-class PI-ALINEA* controllers are adopted with controller parameters optimized according to the framework proposed in Section 3;

Control scheme 3: *EMC-PI-ALINEA* controllers are adopted with controller parameters optimized according to the framework proposed in Section 3 (this is exactly the control scheme described in this article);

Control scheme 4: a finite-horizon optimal control problem is solved to compute the optimal inflows at the entering ramps.

The overall framework corresponding to *Control scheme 2* is shown in Figure 8. Note that, in such scheme, the *Controller Parameter Selector* receives all available state measurements, while the control actions for each controlled on-ramp

are computed according to (24), that is, they are based on the measurements detected immediately downstream the entering ramp.

Before comparing the performance of the four control schemes, let us further detail such schemes. In *Control scheme 1* the following control parameters are adopted for the *Multi-class PI-ALINEA* controller in each controlled ramp $o \in \overline{O}$: $K^1_{\mathrm{P},o} = 100$, $K^2_{\mathrm{P},o} = 50$, $K^1_{\mathrm{R},o} = 33$, $K^2_{\mathrm{R},o} = 6$, $\hat{\rho}^{\sigma}_{o}$=140.

Regarding *Control scheme 2* and *Control scheme 3*, the following considerations hold. Since the simulation starts at 6:00 a.m. and ends at 1:00 p.m., the simulation includes three time windows. Each time window is associated with a recurrent traffic scenario and the presence of the traffic accident requires a non-recurrent traffic scenario associated with the action area and the time window in which the capacity reduction occurs. This leads to the selection of four traffic scenarios that, for the sake of simplicity, for both control schemes are indicated with $\sigma = 1, 2, 3, 4$, as better specified in Table 2. These traffic scenarios are associated with different sets of parameters $\mathbb{K}^{\sigma}$, $\sigma = 1, 2, 3, 4$, the values of which are depicted in Figure 9 for *Control scheme 2* and in Figure 10 for *Control scheme 3*.

Finally, in *Control scheme 4* the flows entering the on-ramps are computed by defining and solving a finite-horizon optimal control problem. In this optimal control problem the objective function $\overline{J}$ to minimize is given by

$$\overline{J} = TTS + \sum_{k=1}^{K\text{-}1} \sum_{c=1}^{C} \sum_{o \in \overline{O}} \omega \left[\overline{q}^{c}_{o}(k) - \overline{q}^{c}_{o}(k-1) \right]^2 \tag{26}$$

where *TTS* is the Total Time Spent, while the second term, weighed with ω, is used to suppress the variations of the control actions over the time horizon. Furthermore, the traffic flow model presented in Section 2 is included by means of

TABLE 2 Traffic scenarios

Scenario name	Scenario type	Start time	End time
$\sigma = 1$	Recurrent	6:00 a.m.	9:00 a.m.
$\sigma = 2$	Recurrent	9:00 a.m.	10:35 a.m.
$\sigma = 3$	Non-recurrent	10:35 a.m.	12:00 a.m.
$\sigma = 4$	Recurrent	12:00 a.m.	1:00 pm

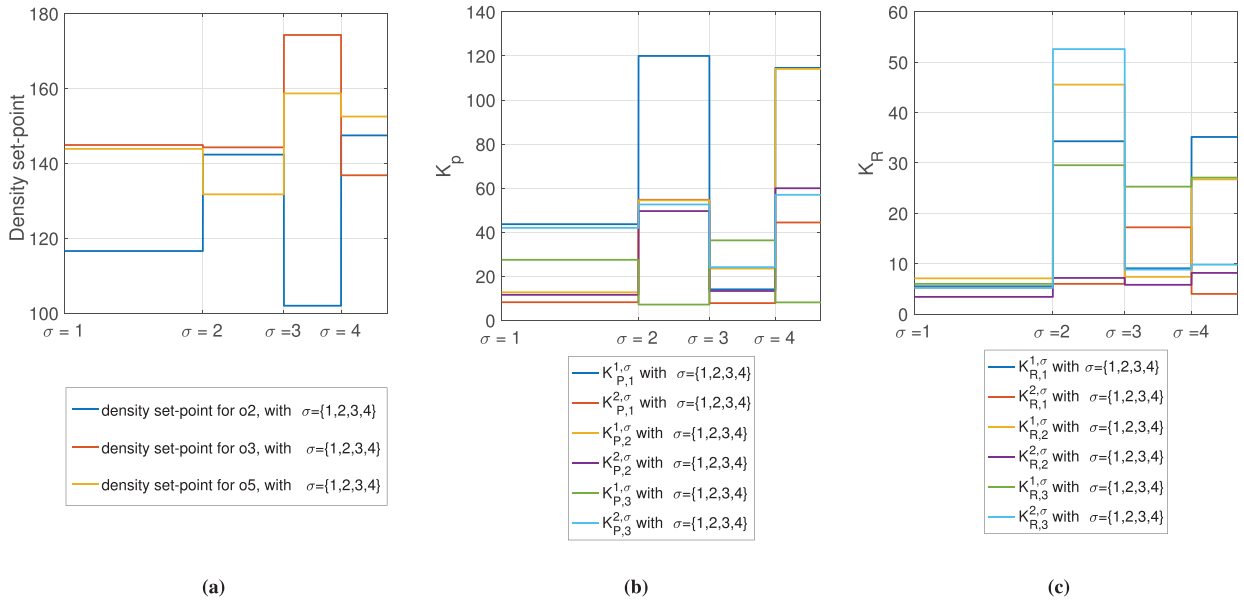

FIGURE 9 Optimal values of density set-points (9a), proportional gain parameters (9b) and integral gain parameters (9c) in *Control scheme 2*

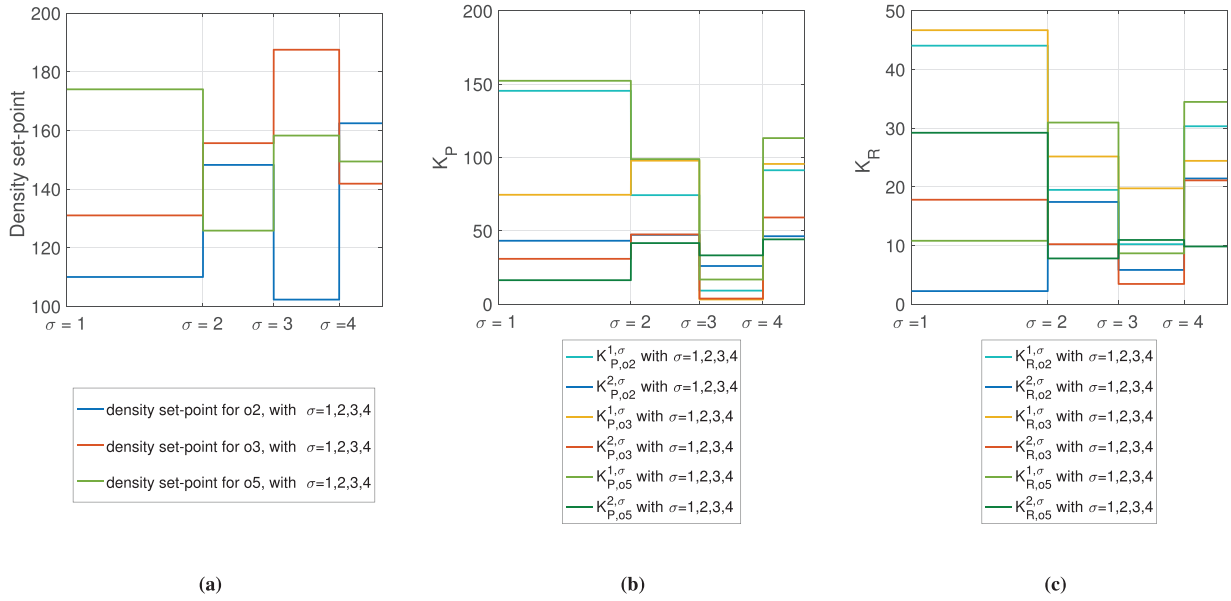

FIGURE 10 Optimal values of density set-points (10a), proportional gain parameters (10b) and integral gain parameters (10c) in *Control scheme 3*

constraints in the optimal control problem. The resulting optimization problem is very complex since it is a highly nonlinear problem with large dimensions. Furthermore, due to the presence of many local minima, the numerical solution of the optimal control problem has been obtained by first performing a global search and then a local search starting the optimal solution obtained with the global search. Both searches have been conducted using the Simulated Annealing algorithm described in Section 3.2. Note that the solution of this optimal control problem for the test case here considered takes several hours, hence it is not applicable in real time but considered only for benchmark purposes. Alternatively to the solution of a finite-horizon optimal control problem, receding-horizon optimal control problems or model predictive control schemes can be used to optimally define the entering flows at the on-ramps. However, it should be noted that the application of such approaches on large-scale freeway networks, although very effective, is still a challenging problem because of their computational burden. Recent works in the literature, such as those proposed in References 40, 41 have recognized that the limits to the applicability of these approaches for real-time control purposes are due, among others, to the complexity of these problems and their computation time that increases rapidly as the size of the freeway network increases.

The application of the four control schemes leads to a substantial improvement in traffic conditions compared to the uncontrolled case. This observation stems from the comparison of the traffic density evolution in the uncontrolled case (Figure 7) with the density evolution for the four controlled cases displayed in Figure 11. By observing these profiles, it is possible to state that the first congestion created by commuter movements during peak hours is completely solved with the application of all control schemes, while the second congestion caused by the traffic accident is partially reduced with a level of effectiveness that depends on the implemented control scheme.

To better analyze the effectiveness of each control scheme, Table 3 shows a comparison in terms of their capability to improve the traffic conditions. Specifically, the columns of the upper part of Table 3 report the values of the Total Time Spent *TTS*, the Total Travel Time *TTT*, the Total Waiting Time *TWT* and the percentage of reduction of *TTS* compared with the uncontrolled case R_{TTS}. The lower part of Table 3 reports the Total Time Spent TTS' computed in the first time window and for the whole network (i.e., during the first congestion), the respective percentage of reduction compared with the uncontrolled case $R_{TTS'}$, the Total Time Spent TTS'' computed for the links and for the time periods involved in the traffic accidents and the corresponding percentage of reduction compared with the uncontrolled case $R_{TTS''}$.

Analyzing these indicators in Table 3, and especially comparing those obtained from the application of *Control scheme 1* and *Control scheme 2*, it can be observed that the *Multi-class PI-ALINEA* controllers with optimized parameters cause a travel time reduction that is higher than the one obtained with the same controllers adopting standard (not optimized) parameters. It is worth noting that the performance produced by *Control scheme 1* could be improved by introducing some

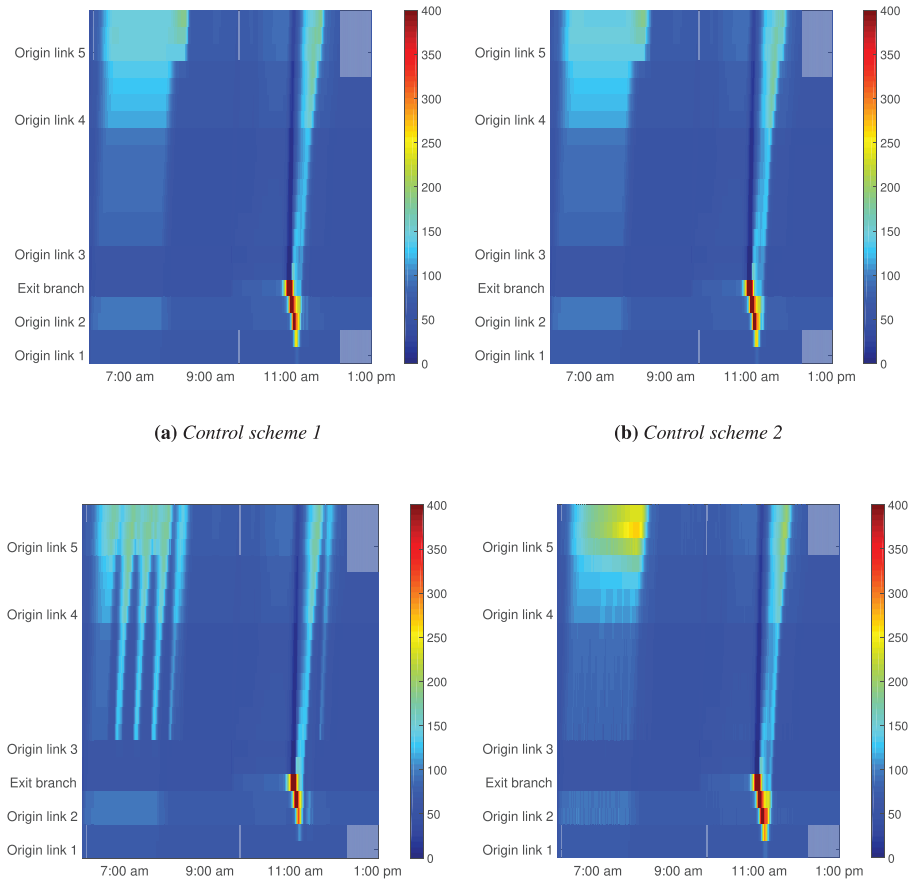

(a) *Control scheme 1*

(b) *Control scheme 2*

(c) *Control scheme 3*

(d) *Control scheme 4*

FIGURE 11 Traffic density evolution in the four control schemes

TABLE 3 Comparison of the control schemes

	TTS [PCE·h]	TTT [PCE·h]	TWT [PCE·h]	R_{TTS} [%]
No control case	10489	10489	-	-
Control scheme 1	9741	8271	1470	7.13
Control scheme 2	9345	8286	1059	10.91
Control scheme 3	8958	8258	700	14.60
Control scheme 4	8835	8569	266	15.77
	TTS' [PCE·h]	$R_{TTS'}$ [%]	TTS'' [PCE·h]	$R_{TTS''}$ [%]
No control case	5644	-	846	-
Control scheme 1	5053	10.47	832	1.65
Control scheme 2	4702	16.69	839	0.87
Control scheme 3	4329	23.3	820	3.07
Control scheme 4	4221	25.21	812	4.02

constraints on the queue lengths at the entering ramps. However, this aspect is not investigated in this article since it is out of the scope of this work.

Moreover, in Table 3 it can also be observed that the application of *Control scheme 3*, in which all local controllers are of *EMC-PI-ALINEA* type, leads to better performance than *Control scheme 1* and *Control scheme 2*. However, the best performance is achieved by applying *Control scheme 4* in which the optimization-based approach is performed, even if this performance is only slightly better than the one obtained with *Control scheme 3*. Note that the parameters adopted in *Control scheme 2* and *Control scheme 3* have been obtained on the basis of scenarios with characteristics that are similar but not identical to the traffic conditions of the case study, making these results even more valuable.

To further compare the four control schemes, it can be useful to analyse the queue lengths at the origin links, as reported in Figure 12. Looking at this figure, it is possible to consider that the *Multi-class PI-ALINEA* controllers with standard parameters in *Control scheme 1* lead to very long queues at the entering on-ramps, corresponding to high waiting times, represented by *TWT*, as reported in Table 3. Again in Figure 12 it is possible to notice that the results obtained from the application of *Control scheme 3* are the closest to the results obtained by solving the optimization problem in *Control scheme 4*.

Specifically, when *Control scheme 1* and *Control scheme 2* are applied, the ramp metering strategy is actuated mainly at origin link o5 creating queues on that on-ramp (see Figure 12a and Figure 12b), hence entailing an overall improvement in the mainstream, as also shown in Figure 13, at the expense of users aiming to access from ramp o5. The *Control scheme 3*, on the other hand, activates ramp metering on both the controlled on-ramps o3 and o5 (see Figure 12c), producing a more effective and fair solution. Even observing the trend of the queues produced in dealing with the congestion created by the traffic accident, it can be noted that *Control scheme 1* and *Control scheme 2* act later than *Control scheme 3*, which turns out to be more performing also in this circumstance. This effectiveness is motivated by the fact that in *Control scheme 3* the control actions are calculated on the basis of traffic conditions detected over the entire action area associated with each controlled origin link and not only on the basis of the measurements taken downstream the on-ramps as in *Multi-class PI-ALINEA*. Of course, the best control actions are those obtained by applying *Control scheme 4*. Analyzing the trends of the queues in Figure 12d it is possible to notice that this control scheme acts in strong

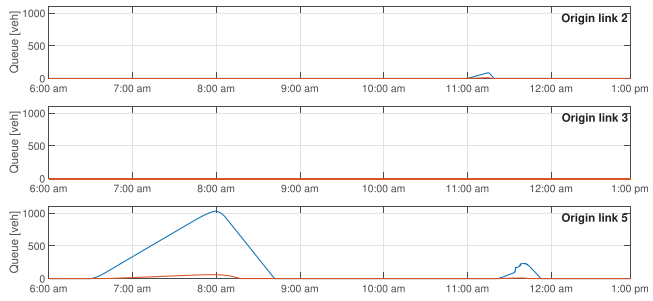

(a) *Control scheme 1*

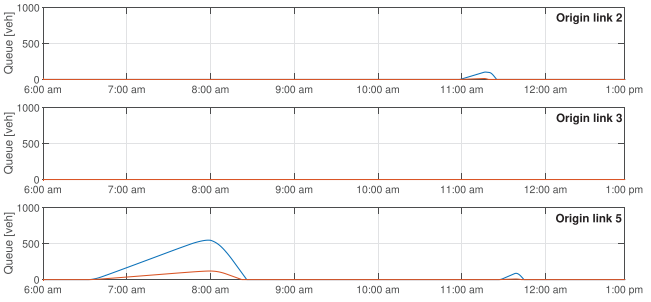

(b) *Control scheme 2*

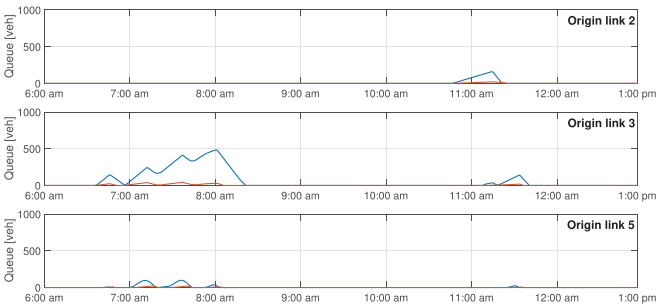

(c) *Control scheme 3*

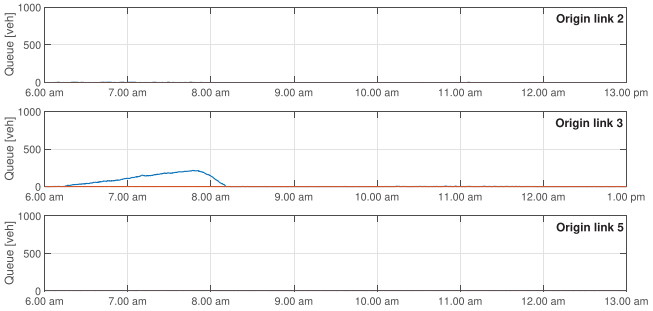

(d) *Control scheme 4*

FIGURE 12 Queue length at the controlled origin links in the four control schemes: blue line for cars, red line for trucks

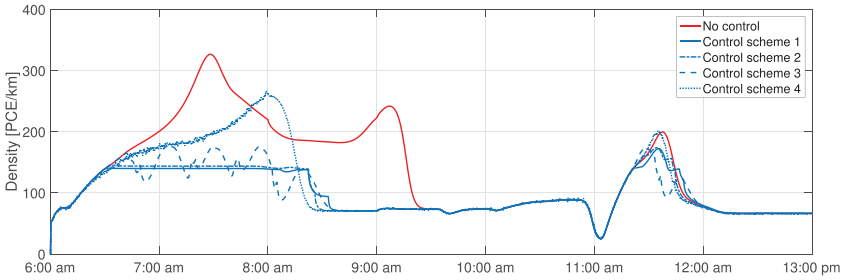

FIGURE 13 Traffic density evolution downstream the origin link o5 in the four control schemes

advance in comparison with the other control schemes producing, at the origin link o5, a queue of shorter length but lasting longer.

Finally, it can be observed that the control scheme proposed in the present article (*Control scheme 3*) provides a performance that is very close to the optimal one (*Control scheme 4*) and, also, is a very effective tool for large-scale and real-time applications, since all the optimization procedures are applied completely offline and, hence, the computational burden does not represent a limitation for the real applicability. Another aspect to consider for the optimal calibration approach is that all the scenarios and the corresponding controller parameters must be saved in a database but the associated memory requirement is not critical for real applications since the size of data to be saved is absolutely compatible with the standard databases used by freeway traffic managers to save historical traffic data.

5 | CONCLUSIONS

This paper proposes an optimization-based calibration approach to define the control parameters of PI controllers adopted to compute the ramp metering flows. The control framework proposed in this work has a general nature and can be applied to different PI regulators. The main peculiarities of this scheme concerns the optimal determination of the controller parameters, since the tuning of the control parameters is particularly crucial to ensure an effective control.

The methodology proposed in this paper is based on offline optimization of these parameters on the basis of recurring or non-recurring traffic scenarios that may occur on the network under consideration. This allows to build a library of parameters from which the most appropriate ones are chosen online on the basis of the traffic conditions actually occurring in the network. As shown in the section dedicated to the description of the simulative results, the adoption of a specific version of the Simulated Annealing algorithm allows to find optimal solutions that are not very sensitive to the choice of the initial solutions adopted and in a rather short computation time. Despite these characteristics, it is not advisable to use this optimization procedure in real time both because it is a stochastic procedure that for some runs could provide inadequate solutions, and because it is not always possible to obtain from the real system all the information needed to solve the optimization problem.

The application of this scheme to a case study has shown that the optimal setting of the controller parameters produces very satisfactory results. In addition, these results have been compared with those obtained from solving an optimal ramp metering control problem. From these experiments it is possible to conclude that the rather simple implementation of the offline controller parameter library and the selection of these parameters online makes this approach workable in real control applications.

DATA AVAILABILITY STATEMENT

The data that support the findings of this study are available by contacting the corresponding author.

ORCID

Cecilia Pasquale https://orcid.org/0000-0002-0760-4769

REFERENCES

1. Ferrara A, Sacone S, Siri S. Ch. 1 Freeway traffic systems. *Freeway Traffic Modelling and Control*. Advances in Industrial Control Series. Springer; 2018:3-23.

2. Papageorgiou M, Papamichail I. Overview of traffic signal operation policies for ramp metering. *Transp Res Rec*. 2008;2047:28-36.
3. Siri S, Pasquale C, Sacone S, Ferrara A. Freeway traffic control: A survey. *Automatica*. 2021;130:109655. http://dx.doi.org/10.1016/j.automatica.2021.109655
4. Kotsialos A, Papageorgiou M. Nonlinear Optimal Control Applied to Coordinated Ramp Metering. *IEEE Transactions on Control Systems Technology*. 2004;12:(6):920-933. http://dx.doi.org/10.1109/tcst.2004.833406
5. Gomes G, Horowitz R. Optimal freeway ramp metering using the asymmetric cell transmission model. *Transp Res C*. 2006;14:244-262.
6. Pasquale C, Papamichail I, Roncoli C, Sacone S, Siri S, Papageorgiou M. Two-class freeway traffic regulation to reduce congestion and emissions via nonlinear optimal control. *Transp Res C*. 2015;55:85-99.
7. Papamichail I, Kotsialos A, Margonis I, Papageorgiou M. Coordinated ramp metering for freeway networks - a model-predictive hierarchical control approach. *Transp Res C*. 2010;18:311-331.
8. Hegyi A, De Schutter B, Hellendoorn H. Model predictive control for optimal coordination of ramp metering and variable speed limits. *Transp Res C*. 2005;13:185-209.
9. Bellemans T, De Schutter B, De Moor B. Model predictive control for ramp metering of motorway traffic: A case study. *Control Engineering Practice*. 2006;14:(7):757-767. http://dx.doi.org/10.1016/j.conengprac.2005.03.010
10. Ferrara A, Sacone S, Siri S. Event-triggered model predictive schemes for freeway traffic control. *Transp Res C*. 2015;58:554-567.
11. Papageorgiou M, Marinaki M, Typaldos P, Makantasis K. *A Feasible Direction Algorithm for the Numerical Solution of Optimal Control Problems*. Dynamic Systems and Simulation Laboratory, Technical University of Crete; 2016.
12. Pasquale C, Anghinolfi D, Sacone S, Siri S, Papageorgiou M. A comparative analysis of solution algorithms for nonlinear freeway traffic control problems. Proceedings of the 9th IEEE International Conference on Intelligent Transportation Systems; 2016:1773-1778.
13. Kotsialos A, Papageorgiou M. A hierarchical ramp metering control scheme for freeway networks. Proceedings of the of IEEE American Control Conference; 2005:2257-2262.
14. Majid H, Hajiahmadi M, De Schutter B, Abouaïssa H & Jolly D Distributed model predictive control of freeway traffic networks: a serial partially cooperative approach. Proceedings of the 17th International IEEE Conference on Intelligent Transportation Systems; 2014:1876-1881.
15. Dabiri A, Kulcsar B. Distributed Ramp Metering—A Constrained Discharge Flow Maximization Approach. *IEEE Transactions on Intelligent Transportation Systems*. 2017;18:(9):2525-2538. http://dx.doi.org/10.1109/tits.2017.2673782
16. Luspay T, Csikós A, Péni T, Varga I, Kulcsár B. Set-based multi-objective control of metered ramps at ring road junctions. *Transp A Transp Sci*. 2020;16(2):337-357.
17. Papageorgiou M, Hadj-Salem H, Blosseville JM. ALINEA: a local feedback control law for on-ramp metering. *Transp Res Rec*. 1991;1320:58-64.
18. Wang Y, Papageorgiou M, Gaffney J, Papamichail I, Guo J. Local ramp metering in the presence of random-location bottlenecks downstream of a metered on-ramp. Proceedings of 13th IEEE Conference on Intelligent Transportation Systems; 2010; 1462-1467.
19. Wang Y, Kosmatopoulos EB, Papageorgiou M, Papamichail I. Local Ramp Metering in the Presence of a Distant Downstream Bottleneck: Theoretical Analysis and Simulation Study. *IEEE Transactions on Intelligent Transportation Systems*. 2014;15:(5):2024-2039. http://dx.doi.org/10.1109/tits.2014.2307884
20. Pasquale C, Sacone S, Siri S, Ferrara A. Supervisory multi-class event-triggered control for congestion and emissions reduction in freeways. Proceedings of the 20th IEEE Intelligent Transportation Systems Conference; 2017:1535-1540.
21. Pasquale C, Sacone S, Siri S, Ferrara A. Hierarchical Centralized/Decentralized Event-Triggered Control of Multiclass Traffic Networks. *IEEE Transactions on Control Systems Technology*. 2021;29:(4):1549-1564. http://dx.doi.org/10.1109/tcst.2020.3016341
22. Pasquale C, Sacone S, Siri S. Multi-class local ramp metering to reduce traffic emissions in freeway systems. Proceedings of the IFAC Workshop on Advances in Control and Automation Theory for Transportation Applications; 2013:43-48.
23. Pasquale C, Sacone S, Siri S, De Schutter B. A multi-class model-based control scheme for reducing congestion and emissions in freeway networks by combining ramp metering and route guidance. *Transp Res C*. 2017;80:384-408.
24. T. Schreiter, H. van Lint & S. Hoogendoorn Multi-class ramp metering: concepts and initial results. Proceedings of the 14th IEEE Conference on Intelligent Transportation Systems; 2011:885-889.
25. Liu S, Hellendoorn H, De Schutter B. Model Predictive Control for Freeway Networks Based on Multi-Class Traffic Flow and Emission Models. *IEEE Transactions on Intelligent Transportation Systems*. 2017;18:(2):306-320. http://dx.doi.org/10.1109/tits.2016.2573306
26. Pasquale C, Sacone S, Siri S. Ramp metering control for two vehicle classes to reduce traffic emissions in freeway systems. Proceedings of the European Control Conference; 2014:2588-2593.
27. Kouvelas A, Saeedmanesh M, Geroliminis N. Enhancing model-based feedback perimeter control with data-driven online adaptive optimization. *Transp Res B*. 2017;96:26-45.
28. Frejo JRD, De Schutter B. Feed-Forward ALINEA: A Ramp Metering Control Algorithm for Nearby and Distant Bottlenecks. *IEEE Transactions on Intelligent Transportation Systems*. 2019;20:(7):2448-2458. http://dx.doi.org/10.1109/tits.2018.2866121
29. Zegeye SK, De Schutter B, Hellendoorn J, Breunesse E.A, Hegyi Andreas. A Predictive Traffic Controller for Sustainable Mobility Using Parameterized Control Policies. *IEEE Transactions on Intelligent Transportation Systems*. 2012;13:(3):1420-1429. http://dx.doi.org/10.1109/tits.2012.2197202
30. Liu S, Sadowska A, Frejo J.R.D, Núñez A, Camacho EF, Hellendoorn H, De Schutter B. Robust receding horizon parameterized control for multi-class freeway networks: A tractable scenario-based approach. *International Journal of Robust and Nonlinear Control*. 2016;26:(6):1211-1245. http://dx.doi.org/10.1002/rnc.3500

31. Papageorgiou M, Blosseville J-M, Hadj-Salem H. Modelling and real-time control of traffic flow on the southern part of Boulevard Périphérique in Paris: Part I: modelling. *Transp Res A*. 1990;24:345-359.
32. Metropolis N, Rosenbluth AW, Rosenbluth MN, Teller AH, Teller E. Equation of state calculations by fast computing machines. *J Chem Phys*. 1953;21:1087-1092.
33. Kirkpatrick S, Gelatt CD, Vecchi MP. Optimization by simulated annealing. *Science*. 1983;220:671-680.
34. Bohachevsky IO, Johnson ME, Stein ML. Generalized Simulated Annealing for Function Optimization. *Technometrics*. 1986;28:(3):209-217. http://dx.doi.org/10.1080/00401706.1986.10488128
35. Anghinolfi D, Canepa E, Cattanei A, Paolucci M. Psychoacoustic Optimization of the Spacing of Propellers, Helicopter Rotors, and Axial Fans. *Journal of Propulsion and Power*. 2016;32:(6):1422-1432. http://dx.doi.org/10.2514/1.b35960
36. Gan G, Ma C, Wu J. *Data Clustering: Theory, Algorithms, and Applications*. Society for Industrial and Applied Mathematics; 2020.
37. Aggarwal CC. *Data Classification: Algorithms and Applications*. CRC Press; 2014.
38. Alpaydin E. *Introduction to Machine Learning*. MIT Press; 2020.
39. Aggarwal CC. *Neural Networks and Deep Learning*. Vol 10. Springer; 2018:978-973.
40. Todorovic U, Frejo JRD, De Schutter B. Distributed MPC for Large Freeway Networks Using Alternating Optimization. *IEEE Transactions on Intelligent Transportation Systems*. 2020;1-10. http://dx.doi.org/10.1109/tits.2020.3028850
41. Frejo JRD, De Schutter B. Logic-Based Traffic Flow Control for Ramp Metering and Variable Speed Limits—Part 1: Controller. *IEEE Transactions on Intelligent Transportation Systems*. 2021;22:(5):2647-2657. http://dx.doi.org/10.1109/tits.2020.2973717

How to cite this article: Pasquale C, Sacone S, Siri S. Optimization of time-varying feedback controller parameters for freeway networks. *Optim Control Appl Meth*. 2022;43(1):65-85. doi: 10.1002/oca.2796